



ELSEVIER

Available at
www.ComputerScienceWeb.com
POWERED BY SCIENCE @ DIRECT®

Pattern Recognition Letters 24 (2003) 393–401

Pattern Recognition
Letters

www.elsevier.com/locate/patrec

Texture classification by multi-model feature integration using Bayesian networks

Yong Huang, Kap Luk Chan *, Zhihua Zhang

*School of Electrical and Electronic Engineering, Nanyang Technological University, Nanyang Avenue,
Singapore 639798, Singapore*

Received 26 February 2002; received in revised form 3 June 2002

Abstract

In this paper, a texture classification method based on multi-model feature integration by Bayesian networks is proposed. Considering that many image textures exhibit both structural and statistical properties, two feature sets based on two texture models—the Gabor model and the Gaussian Markov random field model are used to describe the image properties in both structure and statistics. A Bayesian network classifier is then used to combine these two sets of features along with their individual confidence measures for texture classification. Seventy eight Brodatz textures were used to evaluate the classification performance. The results show that the proposed method is better than that using a single set of features from either model for texture classification.

© 2002 Elsevier Science B.V. All rights reserved.

Keywords: Gaussian Markov random field; Gabor filter; Feature integration; Bayesian networks; Texture classification

1. Introduction

Texture classification is the identification of an observed texture sample as one of the several possible texture classes by using a reliable but computationally attractive texture classifier. The extracted texture features should also efficiently embody as much information as possible about the textural characteristics of the image. Then the classifier can perform classification with minimal error.

Early methods on extraction of texture features were statistical or structural. The statistical meth-

ods characterize a texture by the statistics of the inter-dependence of image pixel gray values. These methods give relatively high recognition accuracy when the image has random looking textured patterns, but not so good for more structured macro-textured patterns. The structural methods assume that a texture is generated by the placement of primitives according to certain placement rules. These methods usually give good results in classifying structural textures. Its recognition accuracy for random textures is not high. Natural textures usually contain both structural and statistical components. Using a single type of features cannot describe such image textures completely.

Recently, some research work on texture description using multi-models or using a unified

* Corresponding author.

E-mail address: eklchan@ntu.edu.sg (K.L. Chan).

model to describe both structural and statistical properties together have been reported. Francos et al. (1993) proposed a unified texture model based on a 2D Wold-like decomposition of the homogeneous random field. Heeger and Bergen (1995) proposed a pyramid-based texture model to synthesize a texture image by matching the texture appearance of given digitized sample. Zhu et al. (1996) proposed a FRAME model that incorporates the responses of a set of well selected filters into a distribution over a random field. These models demonstrated their ability to describe and synthesize a wide variety of textures. Texture classification using multi-model feature integration was also reported recently (Ng et al., 1998; Wang et al., 1998). The integration approaches include what we termed as feature fusion and decision fusion in this paper, which can occur at either of the two stages of feature description and classification, or at both stages. Feature fusion refers to the concatenation of multiple feature sets together into a single feature vector (cf. ‘stacked-vector’ in Benediktsson et al., 1997) which is then input to a classifier. This is a general and simplest way to classify texture image by multi-model feature fusion. However, there are some disadvantages of this method: (1) curse of dimensionality; its dimensionality is higher than that of any component feature vector, and (2) difficulty in feature compatibility; it is hard to lump several feature vectors together due to their diversified forms. For example, some feature values are linearly varying or non-linearly varying or are even circular measures like the degree of angles. In decision fusion, a local decision is performed on each component feature vector. Then these decisions are combined in a decision fusion center. The decision center has a set of algorithms to integrate the individual and local decisions based on each component feature vector. These algorithms are often based on different techniques such as Boolean logic, voting schemes, fuzzy logics, and neural networks.

Conventional classifiers, such as the K-NN, Fisher’s discriminant analysis, and Bayesian quadratic classifiers, can be used for the classification based on a single set of features or a concatenated feature vector (for an introduction and discussions on these methods see Duda et al., 2000; Jain and

Farrokhnia, 1991). A comparison of these conventional classifiers for classification tasks was also reported in (Chen and Huang, 1993). In this paper, two sets of features based on two texture models, the Gabor model and the Gaussian Markov random field (GMRF) model, are used to describe the image properties in both structure and statistics, respectively. Instead of forming a long feature vector with the two sets of features and using a conventional classifier, they are kept as two separate semantically meaningful sets of features, i.e. as two individual feature vectors. Constructing a classifier that can combine these two sets of features is then the main focus of this paper. The texture classification method proposed in this paper is similar to decision fusion. The key feature in the method is that in the classification phase, a Bayesian network is used to represent the relationships among the set of attributes and the corresponding class labels. The Bayesian network classifier combines these sets of features with individual confidence measures. In the Bayesian network, classifications based on each set of features are implicitly achieved by Bayesian quadratic classifiers. The Bayesian network classifier integrates them to give the final classification. Seventy eight texture classes from Brodatz database (Brodatz, 1966) were used for the evaluation of the classification performance by the Bayesian network. The results show that the proposed method is better than that using a single set of features for texture classification.

2. Texture description by multi-model features

The Gabor model and GMRF model are used to extract the features that describe the image in terms of both structure and statistics. These two models have been applied to texture classification and texture segmentation in (Jain and Farrokhnia, 1991; Chen and Huang, 1993). The Gabor model uses a bank of Gabor filters at multiple scales and orientations to extract the properties of a texture image. This model can extract local spatial frequencies which captures the structural properties of the image texture along some directions. The GMRF model assumes that the texture field is stochastic, stationary and satisfies a conditional

independence assumption. It is able to capture the local (spatial) contextual variations in an image and is effective for the analysis and synthesis of random looking textures.

2.1. The Gabor model features

A Gabor filter bank with four scales ($S = 4$): 0.05, 0.1, 0.2 and 0.4 cycles/image-width, and six orientations ($K = 6$) at 0° , 30° , 60° , 90° , 120° and 150° is used. Two Gabor features were extracted from each filtered image, namely, the mean, μ_{mn} ($m = 0, \dots, S - 1$, $n = 0, \dots, K - 1$), and standard deviation, σ_{mn} ($m = 0, \dots, S - 1$, $n = 0, \dots, K - 1$), as in (Manjunath and Ma, 1996). So, $2SK = 48$ features can be extracted, forming a 48-dimensional feature vector

$$\mathbf{F}_g = (\mu_{00}, \sigma_{00} \dots \mu_{(S-1)(K-1)}, \sigma_{(S-1)(K-1)})^t \quad (1)$$

An alternative way to denote the feature vector is

$$\mathbf{F}_g = (f_{00(\mu)}, f_{00(\sigma)} \dots f_{(S-1)(K-1)(\mu)}, f_{(S-1)(K-1)(\sigma)})^t \quad (2)$$

where \mathbf{F}_g is the feature vector representing the structural part of the texture.

2.2. The GMRF model features

A second-order GMRF model is considered for the conditional probability density of the intensity of a given image texture. The mean, $\bar{\mu}$, and the variance, $\bar{\sigma}^2$, of the gray level texture are calculated. The parameters of GMRF model $\Theta = (\theta_1, \theta_2, \theta_3, \theta_4)$ are estimated as in (Kashyap and Chellappa, 1983) using the least square method. The feature vector for the image texture is denoted by

$$\mathbf{F}_m = (\theta_1, \theta_2, \theta_3, \theta_4, \bar{\mu}, \bar{\sigma}^2)^t \quad (3)$$

\mathbf{F}_m is the feature vector that represents the random part of the texture.

3. Bayesian networks for texture classification

3.1. Bayesian networks

Bayesian networks (Pearl, 1988; Jensen, 2001) are probabilistic networks that represent a set of

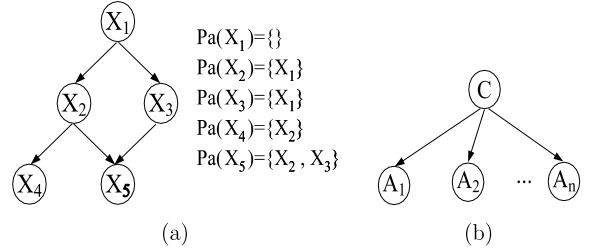


Fig. 1. (a) Example of a Bayesian network, (b) a naive Bayesian classifier.

random variables and the probabilistic relationships among them. A Bayesian network over a set of variables $\mathbf{X} = \{X_1, \dots, X_n\}$ is an annotated directed acyclic graph (DAG) that encodes a joint probability distribution over \mathbf{X} (Fig. 1(a)). Formally, a Bayesian network is a two-tuple $B = (G, L)$. The first component, G , is a DAG whose vertices correspond to the random variables X_1, \dots, X_n , and whose edges represent direct dependencies between the variables. The second component, namely L , represents a set of local conditional probability distributions (CPDs) L_1, \dots, L_n . If x_i denotes some value of the variable X_i and $\mathbf{Pa}(X_i) = \{pa(X_i)\}$ denotes the set of parents of X_i in G , then the CPD for X_i maps possible values x_i of X_i and $pa(X_i)$ of $\mathbf{Pa}(X_i)$ to the conditional probability (density) of x_i given $pa(X_i)$. A Bayesian network B factorizes the joint probability distribution (density) over \mathbf{X} by the product

$$P_B(X_1, \dots, X_n) = \prod_{i=1}^n L_i(X_i | \mathbf{Pa}(X_i)) \quad (4)$$

The factorization is possible thanks to the independence induced by the DAG.

Bayesian networks can be used in classification (Friedman et al., 1997). As an example, let $\mathbf{X} = \{A_1, \dots, A_n, C\}$, where the variables A_1, \dots, A_n are the attributes (features), n is the number of the sets of features and C is the class variable (Fig. 1(b)). Consider a graph structure where the class variable is the root, that is $\mathbf{Pa}(C) = \phi$, and each attribute has the class variable as its unique parent, namely, $\mathbf{Pa}(A_i) = C$, $1 \leq i \leq n$. For this type of graph structure, Eq. (4) yields

$$Pr(A_1, \dots, A_n, C) = Pr(C) \prod_{i=1}^n Pr(A_i | C) \quad (5)$$

From the definition of conditional probability, we get

$$Pr(C|A_1, \dots, A_n) = Pr(C) \prod_{i=1}^n \frac{Pr(A_i|C)}{Pr(A_i)} \quad (6)$$

This is called the *naive Bayesian classifier* (Good, 1950). The attractive properties of the naive Bayesian classifier are the robustness and easy-to-learn—we only need to estimate the CPDs $Pr(C)$ and $Pr(A_i|C)$ for all the attributes. Nonetheless, the naive Bayesian classifier embodies the strong independence assumption that, given the value of the class, attributions are independent of each other.

The main problem considered here is how to learn to perform classification from experience, i.e. given some examples from a domain, learn to classify new instances from the same domain. It will be assumed that the given training examples are labelled with the correct classes.

The underlying regularity assumption used throughout this paper is that the different attributes can be considered as independent (within each class). This assumption is somewhat related to the assumption that samples with many similar attributes often belong to the same class, but not strictly so.

3.2. The classification scheme

The classification scheme by using multiple model feature integration can be expressed as a Bayesian network shown in Fig. 2. It is a multi-layer Bayesian network.

In this figure, F is an input texture image to be classified, F_g and F_m are two feature vectors extracted from two individual texture models. D_{gi} and D_{mi} are two subclasses of the class C_i . D_{gi} corresponds to classification using the feature vector F_g , while D_{mi} corresponds to that using the feature vector F_m . The goal of the classification is to calculate the probability $P(C_i|F_g, F_m)$ and classify the input image F to class C_i^* for which such a probability is maximum, i.e.

$$i^* = \arg \max_i (P(C_i|F_g, F_m)) \quad (7)$$

According to the graph:

$$\begin{aligned} P(C_i|F_g, F_m) &= \sum_{D_{gi}, D_{mi}} P(C_i|D_{gi}, D_{mi}, F_g, F_m) \\ &\quad \times P(D_{gi}|F_g, F_m)P(D_{mi}|F_g, F_m) \\ &= \sum_{D_{gi}, D_{mi}} P(C_i|D_{gi}, D_{mi})P(D_{gi}|F_g) \\ &\quad \times P(D_{mi}|F_m) \end{aligned} \quad (8)$$

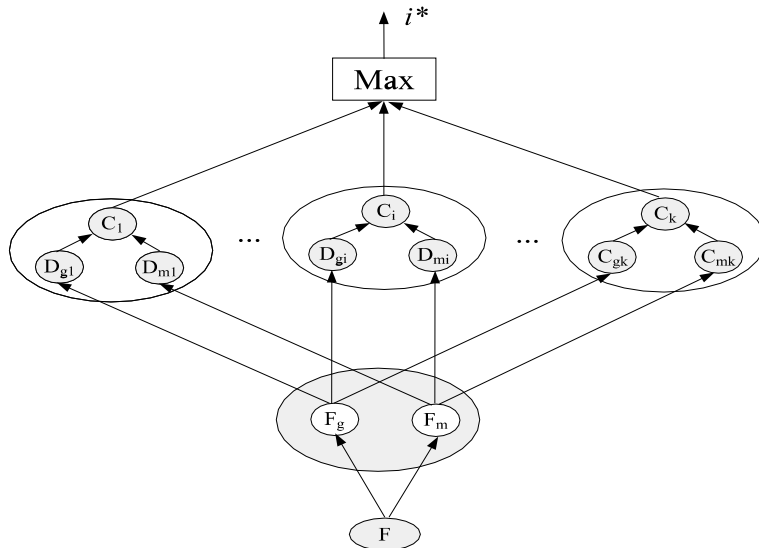


Fig. 2. Classification using multi-model feature integration by Bayesian networks.

where $P(D_{gi}|\mathbf{F}_g)$ and $P(D_{mi}|\mathbf{F}_m)$ are the local classifiers by Gabor model features and GMRF model features, respectively. According to Bayesian theory:

$$P(D_{gi}|\mathbf{F}_g) = \frac{P(\mathbf{F}_g|D_{gi})P(D_{gi})}{P(\mathbf{F}_g)} \quad (9)$$

$$P(D_{mi}|\mathbf{F}_m) = \frac{P(\mathbf{F}_m|D_{mi})P(D_{mi})}{P(\mathbf{F}_m)} \quad (10)$$

As the probabilities $P(\mathbf{F}_g)$ and $P(\mathbf{F}_m)$ are constants for a given training set, we can compare the likelihood using

$$P(D_{gi}|\mathbf{F}_g) = P(\mathbf{F}_g|D_{gi})P(D_{gi}) \quad (11)$$

$$P(D_{mi}|\mathbf{F}_m) = P(\mathbf{F}_m|D_{mi})P(D_{mi}) \quad (12)$$

According to the average majority voting, $P(C_i|D_{gi}, D_{mi})$ is defined as

$$P(C_i|D_{gi}, D_{mi}) \triangleq \frac{\delta(C_i = D_{gi}) + \delta(C_i = D_{mi})}{2} \quad (13)$$

where \triangleq means “defined to be”. $\delta(\cdot)$ is a Kronecker delta function, and it is defined as

$$\delta(x = y) = \begin{cases} 1, & x = y \\ 0, & \text{otherwise} \end{cases} \quad (14)$$

Then we have

$$\begin{aligned} P(C_i|\mathbf{F}_g, \mathbf{F}_m) &= \sum_{D_{gi}, D_{mi}} P(C_i|D_{gi}, D_{mi}) \\ &\quad \times P(D_{gi}|\mathbf{F}_g)P(D_{mi}|\mathbf{F}_m) \\ &= \frac{1}{2} \sum_{D_{gi}, D_{mi}} [\delta(C_i = D_{gi}) + \delta(C_i = D_{mi})] \\ &\quad \times P(D_{gi}|\mathbf{F}_g)P(D_{mi}|\mathbf{F}_m) \\ &= \frac{1}{2} \sum_{D_{gi}, D_{mi}} \delta(C_i = D_{gi})P(D_{gi}|\mathbf{F}_g)P(D_{mi}|\mathbf{F}_m) \\ &\quad + \frac{1}{2} \sum_{D_{gi}, D_{mi}} \delta(C_i = D_{mi})P(D_{gi}|\mathbf{F}_g) \\ &\quad \times P(D_{mi}|\mathbf{F}_m) = \frac{P(D_{gi}|\mathbf{F}_g) + P(D_{mi}|\mathbf{F}_m)}{2} \end{aligned} \quad (15)$$

Then, from Eqs. (11) and (12), the decision rule can be expressed as

$$\begin{aligned} i^* &= \arg \max_i (P(C_i|\mathbf{F}_g, \mathbf{F}_m)) \\ &= \arg \max_i (P(\mathbf{F}_g|D_{gi})P(D_{gi}) + P(\mathbf{F}_m|D_{mi})P(D_{mi})) \end{aligned} \quad (16)$$

where $P(\mathbf{F}_g|D_{gi})$ and $P(\mathbf{F}_m|D_{mi})$ are the conditional probabilities of getting \mathbf{F}_g given D_{gi} and \mathbf{F}_m given D_{mi} . $P(D_{gi})$, $P(D_{mi})$ are the prior probabilities of the two components in class C_i . In the next section, we show how to identify these priors.

In the particular family of texture features, the conditional probabilities, $P(\mathbf{F}_g|D_{gi})$ and $P(\mathbf{F}_m|D_{mi})$, are assumed to be multi-variate normal distributions:

$$\begin{aligned} P(\mathbf{F}_g|D_{gi}) &= \frac{1}{(2\pi)^{d/2} |\Sigma_{gi}|^{1/2}} \\ &\quad \times \exp \left[-\frac{1}{2} (\mathbf{F}_g - \mu_{gi})^T \Sigma_{gi}^{-1} (\mathbf{F}_g - \mu_{gi}) \right] \end{aligned} \quad (17)$$

$$\begin{aligned} P(\mathbf{F}_m|D_{mi}) &= \frac{1}{(2\pi)^{d/2} |\Sigma_{mi}|^{1/2}} \\ &\quad \times \exp \left[-\frac{1}{2} (\mathbf{F}_m - \mu_{mi})^T \Sigma_{mi}^{-1} (\mathbf{F}_m - \mu_{mi}) \right] \end{aligned} \quad (18)$$

where μ_{ji} , $j = (g, m)$ is the mean vector and Σ_{ji} , $j = (g, m)$ is the covariance matrix of class C_i .

It is possible to compute these parameters in a learning procedure with a sufficiently large number of training samples. Let X_i ($i = 1, \dots, M$) be the M feature vectors associated with a set of reference texture samples of type k . The maximum likelihood estimates of the distribution parameters are given by

$$\begin{aligned} \hat{\mu}_k &= \frac{1}{M} \sum_{i=1}^M X_i \\ \hat{\Sigma}_k &= \frac{1}{M} \sum_{i=1}^M (X_i - \hat{\mu}_k)(X_i - \hat{\mu}_k)^T \end{aligned} \quad (19)$$

4. Confidence measures of two feature sets

4.1. Relationship of confidence measure and deterministic energy ratio

In Eq. (16), $P(D_{gi})$ and $P(D_{mi})$ are the prior probabilities of the two subclasses in class C_i . $P(D_{gi})$ and $P(D_{mi})$ can also be regarded as the

confidence measures of characterizing the image as highly structured or relatively unstructured. Their perceptual properties (the visual appearance of the texture being structured pattern or random pattern) is related to the energy partition ratio of these two components. It is found in (Liu, 1997) that the confidence measure of characterizing the image as highly structured or relatively unstructured is related to the deterministic energy ratio α ($\alpha = E_s / (E_s + E_g)$, where E_s and E_g are the energies of the structural and stochastic components in a texture image, respectively). We describe this relationship as a Gibbs distributions, i.e.

$$P(D_{gi}) = \frac{1}{Z} \exp \left(-\frac{1-\alpha}{\alpha T} \right) \quad (20)$$

$$P(D_{mi}) = 1 - P(D_{gi}) \quad (21)$$

where Z is the partition function which normalizes $P(\cdot)$ into a probability distribution, $0 < T < \infty$ is the control parameter. Fig. 3 shows the relationship between the prior probability and deterministic energy ratio α with different values for the control parameter T . We call it the P - α map.

To identify the prior probabilities, we need to obtain the deterministic energy ratio α and determine the control parameter T . In the following, we

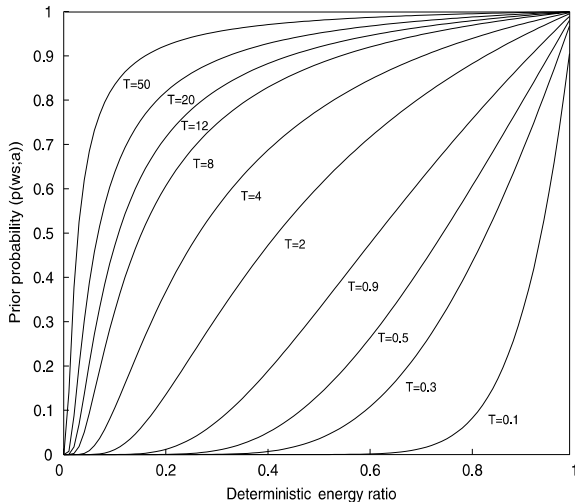


Fig. 3. The relationship between the prior probability and deterministic energy ratio with different values for the control parameter T (P - α map).

will introduce how to calculate the deterministic energy ratio. In Section 5.2, we present the determination of T .

4.2. Texture decomposition and the deterministic energy ratio estimation

The deterministic energy ratio is the ratio of the energy of deterministic component to that of the entire image. To obtain this ratio, the texture image is first decomposed into two components: deterministic component and indeterministic component using a process described in (Huang et al., 2001). The deterministic component corresponds to the structural texture pattern while the indeterministic component corresponds to the random texture pattern.

Let us denote the 2D DFT of an image as $F_y(u, v)$, the corresponding frequency plane as $\Omega((\Omega_s, \Omega_g) \in \Omega)$, where Ω_s is the set of frequencies corresponding to the harmonic peaks and their support regions, and Ω_g is the remaining set of frequencies. The spectrum of the random field can then be decomposed into the deterministic component

$$F_s(u, v) = \begin{cases} F_y(u, v), & (u, v) \in \Omega_s \\ 0, & \text{otherwise} \end{cases} \quad (22)$$

and the indeterministic component

$$F_g(u, v) = \begin{cases} F_y(u, v), & (u, v) \in \Omega_g \\ 0, & \text{otherwise} \end{cases} \quad (23)$$

Using the Parseval's theorem, the energy of deterministic component E_s and the total energy of the texture image E_y can be computed as

$$E_s = \frac{1}{N} \sum_{(u,v) \in \Omega} |F_s(u, v)|^2 \quad (24)$$

and

$$E_y = \frac{1}{N} \sum_{(u,v) \in \Omega} |F_y(u, v)|^2 \quad (25)$$

where N is the total number of pixels in the image.

The deterministic energy ratio is then

$$\alpha = \frac{E_s(u, v)}{E_y(u, v)} \quad (26)$$

Note that $E_y = E_s + E_g$.

5. Experiments

5.1. Database for classification experiment

The texture images used in this experiment are taken from the Brodatz texture album (Brodatz, 1966), in which each of the 112 Brodatz textures is considered to form one texture class. Each class has 200 sample images of size 128×128 sampled from an original 512×512 image. All these 200 sample images are divided into two subsets for training and testing. Each training set consists of 100 images which are sampled from the top half of the original 512×512 texture image, another 100 images are sampled from the bottom half of the texture image for testing. In this paper, an assumption was made that all the images in the database are homogeneous textured patterns. The 200 sampled images will then contain the same homogeneous texture. However, in the collection of Brodatz textures, both homogeneous and heterogeneous textures are present. This produces a negative impact on the texture classification performance. So, the classification experiment was done on 78 homogeneous textures out of the 112 Brodatz textures.

The classification accuracy is calculated from the confusion matrix which contains information about the correct classification and misclassification of all classes. Confusion matrix is a $M \times M$ matrix, where M is the number of classes. For a classification rate of 100%, this matrix should be diagonal.

5.2. Experiment with different control parameters

As we discussed in the previous section that the prior probabilities of the structural and stochastic components are related to the deterministic energy ratio and this relationship is controlled by the control parameter T . Different T values give different curves in the P - α map, and they will influence the classification results. This experiment aims to find the appropriate value of T which can improve the classification results significantly.

As we know, the range of T is $[0, \infty]$. It is impossible to calculate for the full range of T . In this experiment, the values of T are sampled in accordance with the exponential function, i.e. $T = e^t$, where $t = 0, 1, \dots, 10$. Fig. 4(a) shows the correct classification rates (CCRs). This figure illustrates that the classification results are dependent on the control parameter T , which itself is dependent on the image database. Better classification is achieved when T is around 20. Fig. 4(b) shows that when $T = 15$, the CCR is the best (95.54%).

5.3. Comparison experiment

To evaluate the efficiency of the proposed method, results for the classification were calculated based on Gabor and GMRF features alone and various prior probabilities, i.e. (i) equal value $P(D_{gi}) = P(D_{mi}) = 0.5$, (ii) linear relationship with deterministic energy ratio α , $P(D_{gi}) = \alpha$, and (iii) exponential relationship proposed in this paper. The experimental results are shown in Tables 1

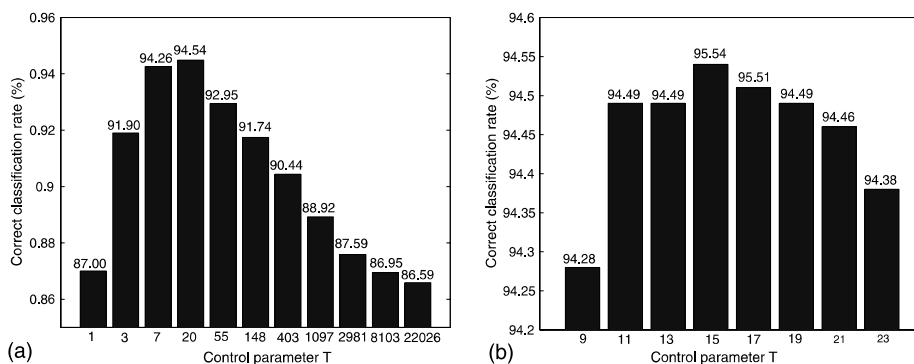


Fig. 4. CCR with different control parameter T . (a) CCR when $T = e^t$, $t = 1, \dots, 10$, (b) CCR when $T = 9, \dots, 23$.

Table 1

Comparison of the average CCR of different method (%)

Method	Gabor	GMRF	$P(D_{gi}) = 0.5$	$P(D_{gi}) = \alpha$	$P(D_{gi}) = e^{-(1-\alpha)/\alpha T}$
CCR	86.44	72.62	91.90	93.51	95.54

Table 2

Comparison of the CCR of each groups (%)

Method	Gabor	GMRF	$P(D_{gi}) = 0.5$	$P(D_{gi}) = \alpha$	$P(D_{gi}) = e^{-(1-\alpha)/\alpha T}$
CCR-group 1	96.20	83.80	95.20	92.60	96.40
CCR-group 2	84.62	68.16	90.75	92.98	93.70
CCR-group 3	88.29	95.43	97.14	99.43	99.14

and 2. Table 1 gives an overview of the average CCR of all the 78 texture classes. As expected, the multi-model feature integration gives better classification result than just using one kind of texture features.

In order to evaluate the effectiveness of the proposed method, the average CCRs for different types of texture images in the database are calculated. Seventy eight homogeneous textures are partitioned into three groups by the deterministic energy ratio α . Group 1 contains 10 textures with $\alpha > 0.6$. The texture images in this group exhibit strong structural property. Group 3 contains seven textures with $\alpha < 0.1$. The texture images in this group exhibit strong random property. The rests are in the group 2, i.e. they exhibit both structural and random appearance.

From the results shown in Table 2, it can be seen that Gabor feature is better than GMRF feature for structural textures, however the GMRF feature is better than Gabor feature for random textures. Combining the Gabor feature and GMRF feature in the texture classification gives better classification results than that just using single type of features. Our proposed method achieve better results in group 1 and group 2. In group 3, it also gives good results.

6. Conclusions

By considering an image texture consisting of both structural and statistical properties, two texture models—Gabor model and GMRF model are

used to extract the features which describe the image by both properties. A Bayesian network is used in the classification to integrate both types of features by maximizing the posterior conditional probability. The Bayesian prior probabilities are regarded as the confidence measures of characterizing the texture being structured and/or unstructured. Gibbs distribution assumption is made to model this probability associated with deterministic energy ratio α . Experimental results indicate that this method improves the classification accuracy significantly for a wide variety of texture types. It shows the integration of different types of features representing the structured and random properties performs better classification than using a single type of features.

References

- Benediktsson, J.A., Sveinsson, J.R., Swaine, P.H., 1997. Hybrid consensus theoretic classification. *IEEE Trans. Geosci. Remote Sensing* 35 (4), 833–843.
- Brodatz, P., 1966. *Textures: A Photographic Album for Artists and Designers*. Dover.
- Chen, C.C., Huang, C.L., 1993. Markov random fields for texture classification. *Pattern Recogn. Lett.* 14, 907–914.
- Duda, R.O., Hart, P.E., Stork, D.G., 2000. *Pattern Classification*, second ed. John Wiley & Sons, New York.
- Francois, J.M., Meiri, A.Z., Porat, B., 1993. A unified texture model based on a 2-D Wold-like decomposition. *IEEE Trans. Signal Proces.* 41 (8), 2665–2678.
- Friedman, N., Geiger, D., Goldszmidt, M., 1997. Bayesian network classifiers. *Mach. Learn.* 29, 131–163.
- Good, I.J., 1950. *Probability and the Weighing of Evidence*. Charles Griffin, London.

- Heeger, D.J., Bergen, J.R., 1995. Pyramid-based texture analysis/synthesis. In: *Proceedings of IEEE International Conference on Image Processing*, Vol. 3, pp. 648–651.
- Huang, Y., Chan, K.L., Huang, Z.Y., 2001. Harmonic extraction based on higher order statistics spectrum decomposition for a unified texture model. In: *Proceedings of IEEE International Conference on Computer Vision*, Vol. 2, pp. 245–250.
- Jain, A.K., Farrokhnia, F., 1991. Unsupervised texture segmentation using Gabor filters. *Pattern Recogn.* 24 (12), 1167–1186.
- Jensen, F.V., 2001. *Bayesian networks and decision graphs*. Springer-Verlag, Berlin.
- Kashyap, R.L., Chellappa, R., 1983. Estimation and choice of neighbors in spatial interaction models of images. *IEEE Trans. Inform. Theory* IT-29, 60–72.
- Liu, F., 1997. *Modeling spatial and temporal textures*. Ph.D. thesis, MIT.
- Manjunath, B.S., Ma, W.Y., 1996. Texture features for browsing and retrieval of image data. *IEEE Trans. Pattern Anal. Mach. Intell.* 18 (8), 837–842.
- Ng, L.S., Nixon, M.S., Carter, J.N., 1998. Texture classification using combined feature sets. In: *IEEE Southwest Symposium on Image Analysis and Interpretation*, pp. 103–108.
- Pearl, J., 1988. *Probabilistic reasoning in expert system: networks of plausible inference*. Morgan Kaufmann, San Mateo, CA.
- Wang, L., Liu, J., Li, S.Z., 1998. Texture classification using wavelet decomposition with Markov random field model. In: *Proceedings 14th International Conference on Pattern Recognition*, Vol. 2, pp. 1613–1615.
- Zhu, S.C., Wu, Y., Mumford, D., 1996. FRAME: filters, random fields and minimax entropy-towards a unified theory for texture modeling. In: *Proceedings of IEEE International Conference on Computer Vision and Pattern Recognition*, pp. 686–693.